PERCOLATION COMPOSITES: LOCALIZATION OF SURFACE PLASMONS AND ENHANCED OPTICAL NONLINEARITIES

V. A. Podolskiy, A. K. Sarychev, and Vladimir M. Shalaev

Department of Physics, New Mexico State University, Las Cruces, NM 88003, U.S.A.

In random metal-dielectric composites near the percolation threshold surface plasmons are localized in small nanometer-sized areas, hot spots, where the local field can exceed the applied field by several orders of magnitude. The high local fields result in dramatic enhancement of optical responses, especially, nonlinear ones. The local-field distributions and enhanced optical nonlinearities are described using the scale renormalization. A theory predicts that the local fields consist of spatially separated clusters of sharp peaks representing localized surface plasmons. Experimental observations are in good accord with theoretical predictions. The localization of plasmons maps the Anderson localization problem described by the random Hamiltonian with both on- and off-diagonal disorder. A feasibility of nonlinear surface-enhanced spectroscopy of single molecules and nanocrystals on percolation films is shown.

I. Introduction

Metal-dielectric composites attract much attention because of their unique optical properties, which are significantly different from those of constituents forming the composite.[1–3] Semicontinuous metal films can be produced by thermal evaporation or sputtering of metal onto an insulating substrate. First, in the growing process, small metallic grains are formed on the substrate. A typical size a of a metal grain is about 5 nm to 50 nm. As the film grows, the metal filling factor increases and coalescence occurs,

C.M. Soukoulis (ed.), Photonic Crystals and Light Localization in the 21st Century, 567–575.

so that irregularly shaped self-similar clusters (fractals) are formed on the substrate. The concept of scale-invariance (fractality) plays an important role in description of various properties of percolation systems.[2,4] The sizes of the fractal structures diverge in the vicinity of the percolation threshold, where an "infinite" percolation cluster of metal is eventually formed, representing a continuous conducting path between the ends of a sample. At the percolation threshold the metal-insulator transition occurs in the system. At higher surface coverage, the film is mostly metallic, with voids of irregular shape. With further coverage increase, the film becomes uniform.

In random metal-dielectric films, surface-plasmon excitations are localized in small nanometer-scale areas referred to as "hot spots".[2,5,6] As discussed below, the localization can be attributed to the Anderson localization of plasmons in semicontinuous metal films near a percolation threshold (in this case, referred to as percolation films). The electromagnetic energy is accumulated in the hot spots associated with localized plasmons, leading to the local fields that can exceed the intensity of the applied field by four to five orders of magnitude. The high local fields in the hot spots also result in dramatically enhanced *nonlinear* optical responses proportional to the local field raised to a power greater than one.

Below, we consider a simple scaling approach explaining the extremely inhomogeneous field distribution and giant optical nonlinearities of fractal composites. We also show a great potential of percolation films for surface-enhanced local spectroscopy of single molecules and nanocrystals.

II. Scaling in the local-field distribution

For the films concerned, gaps between metal grains are filled by a dielectric substrate so that a semicontinuous metal film can be thought of as a $2d$ array of metal and dielectric grains randomly distributed over the plane. The dielectric constant of a metal can be approximated by the Drude formula

$$\epsilon_m = \epsilon_b - (\omega_p/\omega)^2/(1 + i\omega_\tau/\omega), \tag{1}$$

where ϵ_b is the interband contribution, ω_p is the plasma frequency, and ω_τ is the plasmon relaxation rate ($\omega_\tau \ll \omega_p$). In the high-frequency range considered here, losses in metal grains are relatively small, $\omega_\tau \ll \omega$. Therefore, the real part ϵ'_m of the metal dielectric function ϵ_m is much larger (in modulus) than the imaginary part ϵ''_m, i.e., the loss parameter κ is small, $\kappa = \epsilon''_m/|\epsilon'_m| \cong \omega_\tau/\omega \ll 1$. We note that ϵ'_m is negative for frequencies ω less than the renormalized plasma frequency,

$$\tilde{\omega}_p = \omega_p/\sqrt{\epsilon_b}. \tag{2}$$

It is instructive to consider first the special case of $-\epsilon'_m = \epsilon_d$, where $\epsilon_m \equiv \epsilon'_m + i\epsilon''_m$ and ϵ_d are the dielectric constants of the metallic and dielectric components, respectively. The condition $-\epsilon'_m = \epsilon_d$ corresponds to the resonance of individual metal particles in a dielectric host, in the two-dimensional case. For simplicity, we also set $-\epsilon_m = \epsilon_d = 1$, which can always be done by simply renormalizing the corresponding quantities.

It can be shown that the field distribution on a percolation film at $-\epsilon_m = \epsilon_d = 1$ formally maps the Anderson metal-insulator transition problem.[2,5,6] In accord with this,

the field potential representing plasmon modes of a percolation film must be characterized by the same spatial distribution as the electron wavefunction in the Anderson transition problem. Such mathematical equivalence of the two physically different problems stems from the fact that the current conservation law for a percolation film acquires (when written in the discretized form) the form of the Kirchhoff's equations, which, in turn, (when written in the matrix form) become identical to the equations describing the Anderson transition problem.[6] The corresponding Kirchhoff Hamiltonian for the field-distribution problem is given by a matrix with random elements which can be expressed in terms of the dielectric constants for metal and dielectric bonds of the lattice representing the film. In this matrix, the values $\epsilon_m = -1$ and $\epsilon_d = 1$ appear in the matrix elements with probability p and $(1-p)$, respectively (where p is the metal filling factor given at percolation by $p = p_c$, with $p_c = 1/2$ for a self-dual system). In such a form, the Kirchhoff Hamiltonian is characterized by the random matrix, similar to that in the Anderson transition problem, with both on- and off-diagonal disorder. Based on this mathematical equivalence, it was concluded in[2,5,6] that the plasmons in a percolation film can experience the Anderson-type localization within small areas, with the size given by the Anderson length ξ_A. For the most localized plasmon modes, ξ_A can be as small as the size of one grain a.

Below we develop a simple scaling approach that explains the non-trivial field distribution predicted and observed in percolation films. This scale-renormalization method supports main conclusions of a rigorous (but tedious) theory of Refs.[2,5,6] and has a virtue of being simple and clear, which is important for understanding and interpretation of future experiments.

First, we estimate the field in the hot spots for the considered case of $-\epsilon'_m = \epsilon_d$. Hereafter we use the sign * (not to be confused with complex conjugation) to indicate that the quantity concerned is given for the considered case of $-\epsilon'_m/\epsilon_d$ (with $\epsilon_d \sim 1$); for ξ_A, however, we omit this sign since this quantity always refers to the case of $-\epsilon'_m/\epsilon_d$.

Since at the optical frequencies ϵ'_m is negative, metal particles can be roughly thought of as inductor-resistor $(L-R)$ elements, whereas the dielectric gaps between the particles can be treated as capacitive (C) elements. Then, the condition $\epsilon'_m = -\epsilon_d$ means that the conductivities of the $L-R$ and C elements are equal in magnitude and opposite in sign, i.e., there is a resonance in the equivalent $L-R-C$ circuit corresponding to individual particles.

The local field in resonating particles is enhanced by the resonance quality-factor Q which is the inverse of the loss-factor, $Q = \kappa^{-1}$, so that

$$E_m^* \sim E_0 \kappa^{-1} \left(a/\xi_A\right)^2, \tag{3}$$

where the factor $(a/\xi_A)^2$ takes into account that the resonating mode is localized within ξ_A. The resonant modes excited by a monochromatic light represent only the fraction κ of all the modes so that the average distance (referred to as the field correlation length ξ_e^*) between the field peaks is given by

$$\xi_e^* \sim a/\sqrt{\kappa} \gg \xi_A. \tag{4}$$

Note that the field peaks associated with the resonance plasmon modes represent in fact the normal modes, with the near-zero eigennumbers, of the Kirchhoff's Hamiltonian discussed above.[2,6] These modes are strongly excited by the applied field and seen as giant field fluctuations on the surface of the film.

Now we turn to the important case of the "high contrast," with $|\epsilon_m| \gg \epsilon_d$, that corresponds to the long-wavelength part of the spectrum where the local-field enhancement can be especially strong. From basic principles of Anderson localization,[2] it is clear that a higher contrast favors localization so that plasmon modes are expected to be localized in this case as well.

It is clear that at $|\epsilon_m| \gg \epsilon_d$ individual metal particles cannot resonate. We can renormalize, however, the high-contrast system to the case of $-\epsilon'_m = \epsilon_d$ considered above by formally "dividing" the film into square elements of the special resonant size

$$l_r = a\left(|\epsilon_m|/\epsilon_d\right)^{\nu/(t+s)} \tag{5}$$

and considering these squares as new renormalized elements of the film. Using the known scaling dependences[1,4] for "metal" and "dielectric" squares of size l (which, respectively, do or do not contain a metal continuous path through the square):

$$\epsilon_m(l) \sim (l/a)^{-t/\nu}\epsilon_m \tag{6}$$

and

$$\epsilon_d(l) \sim (l/a)^{s/\nu}\epsilon_d, \tag{7}$$

we obtain the dielectric constants of the renormalized elements with the size $l = l_r$, equal in magnitude and opposite in sign, i.e.,

$$-\epsilon_m(l_r) = \epsilon_d(l_r). \tag{8}$$

Thus, for these renormalized elements of the size l_r, there is a resonance similar to the resonance in the $R-L-C$ circuit describing individual metal particles in a dielectric host. In this case, however, some effective (renormalized) $R-L-C$ circuits represent the resonating square elements.

For a two-dimensional percolation film, the critical exponents are given by $t \approx s \approx \nu \approx 4/3$; they represent the percolation critical exponents for conductivity, dielectric constant, and percolation correlation length, respectively.[1,4]

In the renormalized system, the estimate obtained above for field peaks still holds. Since the electric field and eigenfunction both scale as l_r we arrive at the conclusion that in the high-contrast system (with $|\epsilon_m| \gg \epsilon_d$), the field maxima are estimated as

$$E_m \sim (l_r/a)E_m^* \sim E_0\kappa^{-1}(l_r/a)(a/\xi_A)^2 \sim E_0\kappa^{-1}\left(l_r/\xi_A\right)^2 \sim E_0(a/\xi_A)^2|\epsilon_m|^{3/2}\Big/\left(\epsilon_d^{1/2}\epsilon_m''\right). \tag{9}$$

The light-induced eigenmodes in the high-contrast system are separated, on the average, by the distance ξ_e that exceeds the mode separation ξ_e^* at $\epsilon_m = -\epsilon_d$ by factor l_r/a,

$$\xi_e \sim (l_r/a)\xi_e^* \sim l_r/\sqrt{\kappa} \sim a|\epsilon_m|/\sqrt{\epsilon_m''\epsilon_d}. \tag{10}$$

For a Drude metal at $\omega \ll \omega_p$, the local field peaks, according to (1) and (9) are given by

$$E_m/E_0 \sim \epsilon_d^{-1/2}(a/\xi_A)^2\left(\omega_p/\omega_\tau\right), \tag{11}$$

and the distance between the excited modes (10) is estimated as

$$\xi_e \sim a\omega_p/\sqrt{\epsilon_d \omega \omega_\tau}. \tag{12}$$

Figure 1 illustrates the above described renormalization of the field peaks and their spatial separations at the transition between the reference (renormalized) system with $-\epsilon_m = \epsilon_d = 1$ and the high-contrast system of $|\epsilon_m/\epsilon_d| \gg 1$.

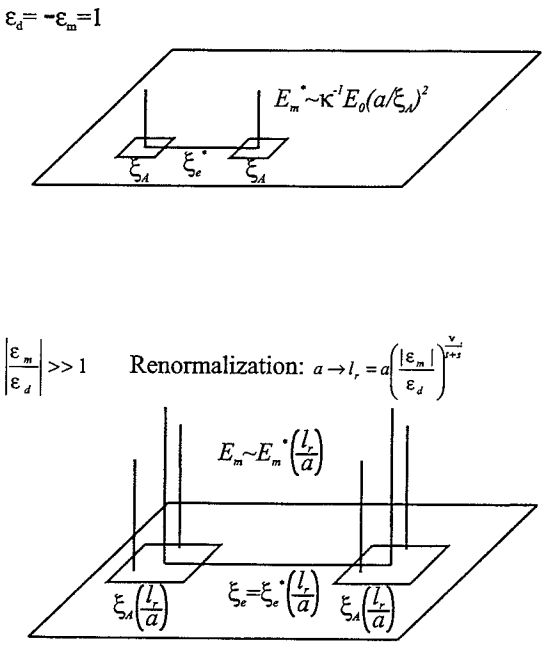

FIG. 1. Renormalization of the field distribution at transition between the reference case with $-\epsilon_m/\epsilon_d = 1$ and the high-contrast case of $-\epsilon_m/\epsilon_d \gg 1$.

As follows from the figure, largest local fields of the amplitude E_m result from excitation of the resonant clusters of the size l_r. At $-\epsilon_m = \epsilon_d = 1$, we have $l_r = a$ (see (5)), as in the reference system. With increasing wavelength (and thus the contrast $|\epsilon_m|/\epsilon_d$), the resonant size l_r and distance ξ_e between the resonating modes both increase.

The above results have a clear physical interpretation and can be also obtained from the following complementary considerations. Let us consider two metal clusters, with conductance $\Sigma_m = -i(a/4\pi)\omega\epsilon_m(l)$, separated by a dielectric gap, with the conductance $\Sigma_d = -i(a/4\pi)\omega\epsilon_d(l)$, as shown in Fig. 2a. The clusters and the gap are both of a size l, and $\epsilon_m(l)$ and $\epsilon_d(l)$ are defined in (6) and (7), respectively. The equivalent conductance Σ_e for Σ_m and Σ_d in series is given by $\Sigma_e = \Sigma_m\Sigma_d/(\Sigma_m + \Sigma_d)$ and the current j through the system is $j = \Sigma_e E_0 l$. The local field, however, is strongly inhomogeneous and the largest field occurs at the point of the close approach between the clusters, where the separation between clusters can be as small as a; then, the maximum field E_m is estimated as $E_m = (j/\Sigma_d)/a \sim E_0(l/a)/\left[1 + (l/a)^{(t+s)/\nu}\epsilon_d/\epsilon_m\right]$ (where we used Eqs. (6) and (7)). For the "resonant" size $l = l_r$, the real part of the denominator in the expression for E_m becomes zero, and the field E_m reaches its maximum, where it is estimated as $E_m/E_0 \sim \kappa^{-1}(l_r/a)$.

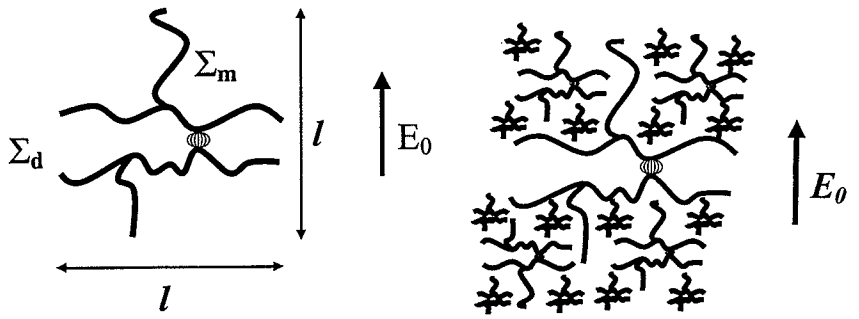

FIG. 2. **(a):** A typical element of a percolation film consisting of two conducting metal clusters with a dielectric gap in between. **(b):** Different resonating elements of a percolation film at different wavelengths.

In the obtained estimate we assumed, for simplicity, that $\xi_A \sim a$ and, in this limit, we reproduced the result (9). In order to obtain the "extra-factor" $(a/\xi_A)^2$ of (9), we take into account that the localization area for the field is ξ_A rather than a, so that the field peak is "spread over" for the distance ξ_A. With this correction we immediately arrive at the formula (9).

It is clear that for any frequency of the applied field ω there are always resonant clusters of the size (5)

$$l = l_r(\omega) \sim a(\omega/\tilde{\omega}_p)^{2\nu/(t+s)}, \tag{13}$$

where the local field reaches its maximum E_m. The resonant size l_r increases with the wavelength. It is important that at percolation, the system is scale-invariant so that all possible sizes needed for the resonant excitation are present, as schematically illustrated in Fig. 1b. At some large wavelength, only large clusters of appropriate sizes resonate leading to field peaks at the points of close approach between the metal clusters; with a decrease of the wavelength of the applied field, the smaller clusters begin to resonate, whereas the larger ones (as well as the smaller ones) are off the resonance, as shown in Fig. 1b.

We can also estimate the number $n(l_r)$ of field peaks within one resonating square of the size l_r. In the high-contrast system (with $|\epsilon_m/\epsilon_d| \gg 1$) each field maximum of the renormalized system (with $|\epsilon_m/\epsilon_d| = 1$) splits into $n(l_r)$ peaks of the E_m amplitude located along a dielectric gap in the "dielectric" square of the l_r size (see Figs. 1 and 2). The gap "area" scales as the capacitance of the dielectric gap, so must do the number of field peaks in the resonance square. Therefore, we estimate that

$$n(l_r) \propto (l_r/a)^{s/\nu_p}. \tag{14}$$

In accordance with the above considerations, the average (over the film surface) intensity of the local field is enhanced as

$$\left\langle \left| \frac{E}{E_0} \right|^2 \right\rangle \sim (E_m/E_0)^2 n(l_r)(\xi_A/\xi_e)^2 \sim (a/\xi_A)^2 |\epsilon_m|^{3/2} \Big/ (\epsilon_m'' \epsilon_d), \tag{15}$$

where we used (5), (10), and (14) and the critical exponents $t = s = \nu = 4/3$.

In Fig. 3, we also show the simulated field distribution on a silver-glass percolation film at two different wavelengths. In accordance with the consideration above, we see that the local field distribution consists of clusters of very sharp peaks with the spatial separation increasing with the wavelength. Qualitatively similar field distribution was detected in recent experiments[5] using scanning near-field optical microscopy.

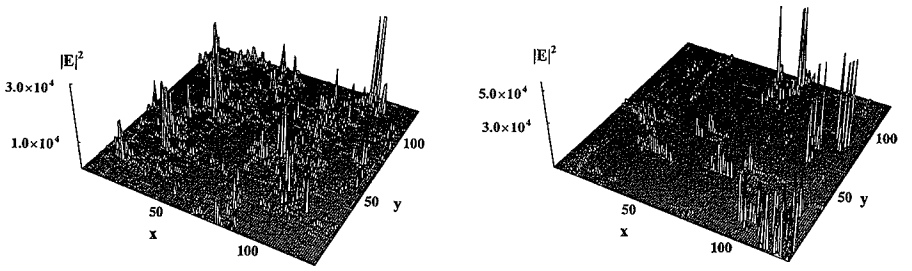

FIG. 3. Local field distribution on silver-glass percolation film at different wavelengths; **(a):** $\lambda = 1.5\mu m$ and **(b):** $\lambda := 10\mu m$.

Thus, using simple arguments based on the scaling dependences of $\epsilon_m(l)$ and $\epsilon_d(l)$ on l and the resonance condition $-\epsilon_m(l_r) = \epsilon_d(l_r)$, one can define the renormalization procedure that allows one to re-scale the "high-contrast" system to the renormalized one with $-\epsilon_m = \epsilon_d = 1$.

Below, we show that the enhanced local-field in the hot spots result in giant enhancement of *nonlinear* optical responses of semicontinuous films.

III. Enhanced optical nonlinearities

In general, we can define the high-order field moments as

$$M_{n,m} = \frac{1}{S E_0^m \left|E_0\right|^n} \int \left|E\left(\mathbf{r}\right)\right|^n E^m\left(\mathbf{r}\right) d\mathbf{r}, \tag{16}$$

where, as above, E_0 is the amplitude of the external field and $E(\mathbf{r})$ is the local field (note that $E^2\left(\mathbf{r}\right) \equiv \mathbf{E}\left(\mathbf{r}\right) \cdot \mathbf{E}\left(\mathbf{r}\right)$). The integration is over the entire surface S of the film.

The high-order field moment $M_{2k,m} \propto E^{k+m} E^{*k}$ represents a nonlinear optical process in which, in one elementary act, $k+m$ photons are added and k photons are subtracted.[7] This is because the complex conjugated field in the general expression for the nonlinear polarization implies photon subtraction so that the corresponding frequency enters the nonlinear susceptibility with the minus sign.[7] Below, we show that the enhancement is significantly different for nonlinear processes with photon subtraction in comparison with those where all photons are entering the nonlinear susceptibility with the sign plus. Enhancement of the Kerr optical nonlinearity G_K (see below) is equal to $M_{2,2}$, second harmonic generation (SHG) and third harmonic generation (THG) enhancements are given by $|M_{0,2}|^2$ and $|M_{0,3}|^2$, respectively, and surface-enhanced Raman

scattering (SERS) is represented by $M_{4,0}$.

The high-order moments of the local field in $d = 2$ percolation films can be estimated as $M_{n,m} \sim (E_m/E_0)^{n+m} n(l_r)(\xi_A/\xi_e)^2$. Using the scaling formulas (5)-(14) for the field distribution, we obtain the following estimate for the field moments

$$M_{n,m} \sim \left(\frac{E_m}{E_0}\right)^{n+m} \frac{(l_r/a)^{s/\nu}}{(\xi_e/\xi_A)^2} \sim \left(\frac{|\epsilon_m|^{3/2}}{(\xi_A/a)^2 \epsilon_d^{1/2} \epsilon_m''}\right)^{n+m-1}, \tag{17}$$

for $n + m > 1$ and $n > 0$ (where, we took into account that for two-dimensional percolation composites, the critical exponents are given by $t \cong s \cong \nu \cong 4/3$).

Since $|\epsilon_m| \gg \epsilon_d$ and the ratio $|\epsilon_m| / \epsilon_m'' \gg 1$, the moments of the local field are very large, i.e., $M_{n,m} \gg 1$, in the visible and infrared spectral ranges. Note that the first moment, $M_{0,1} \simeq 1$, corresponds to the equation $\langle \mathbf{E}(\mathbf{r}) \rangle = \mathbf{E}_0$.

Consider now the moments $M_{n,m}$ for $n = 0$, i.e., $M_{0,m} = \langle E^m(\mathbf{r}) \rangle / (E_0)^m$. In the renormalized system where $\epsilon_m(l_r)/\epsilon_d(l_r) \cong -1 + i\kappa$, the field distribution coincides with the field distribution in the system with $\epsilon_d \simeq -\epsilon_m' \sim 1$. In that system, field peaks, E_m^*, being different in phase, cancel each other, resulting in the moment $M_{0,m}^* \sim O(1)$.[6] In transition to the original system, the peaks increase by the factor l_r, leading to an increase in the moment $M_{0,m}$. Then, using (5), (10), and (14), we obtain the following equation for the moment:

$$M_{0,m} \sim M_{0,m}^* (l_r/a)^m \left(\frac{n(l_r)}{(\xi_e/a)^2}\right) \sim \kappa (l_r/a)^{m-2+s/\nu} \sim \frac{\epsilon_m'' |\epsilon_m|^{(m-3)/2}}{\epsilon_d^{(m-1)/2}}, \tag{18}$$

for $m > 1$ (where we again used the critical exponents $t \cong s \cong \nu \cong 4/3$).

For a Drude metal (1) and $\omega \ll \omega_p$, from (17) and (18), we obtain

$$M_{n,m} \sim \epsilon_d^{(1-n-m)/2} (a/\xi_A)^{2(n+m-1)} (\omega_p/\omega_\tau)^{n+m-1}, \tag{19}$$

for $n + m > 1$ and $n > 0$, and

$$M_{0,m} \sim \epsilon_d^{(1-m)/2} \left(\frac{\omega_p^{m-1} \omega_\tau}{\omega^m}\right), \tag{20}$$

for $m > 1$.

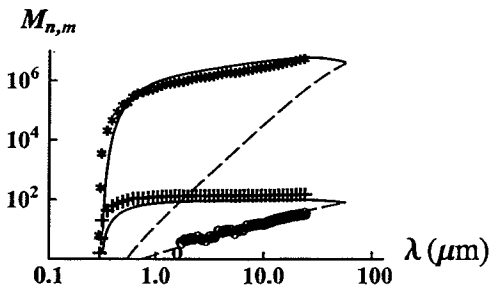

FIG. 4. Average enhancement of the high-order field moments $M_{n,m}$ in a percolation silver-glass two-dimensional film as a function of the wavelength: $M_{4,0}$ (scaling formula (17) - upper solid line and numerical simulations - *); $M_{0,4}$ (scaling formula (18) - upper dashed line); $M_{2,0}$ (scaling formula (17) - lower solid line and numerical simulations - +); $M_{0,2}$ (scaling formula (18) - lower dashed line and numerical simulations - 0).

Note that for all moments the maximum in (19) and (20) is approximately the same (if $\xi_A \sim a$), so that

$$M_{n,m}^{(\max)} \sim \epsilon_d^{(1-n-m)/2} \left(\frac{\omega_p}{\omega_\tau}\right)^{n+m-1} \tag{21}$$

However, in the spectral range $\omega_p \gg \omega \gg \omega_\tau$, moments $M_{0,m}$ gradually increase with the wavelength and the maximum is reached only at $\omega \sim \omega_\tau$, whereas the moments $M_{n,m}$ (with $n > 1$) reach this maximum at much shorter wavelengths (roughly, at $\omega \approx \tilde{\omega}_p/2$) and remain almost constant in the indicated spectral interval. This conclusion is supported by the numerical simulations for silver-glass percolation films shown in Fig. 4; one can see that the above scaling formulas are in good accord with the simulations.

For silver-glass percolation films, with $\omega_p = 9.1$ ev and $\omega_\tau = 0.021$ ev, we find that the average field-enhancement can be as large as $G_{RS} \sim M_{4,0} \sim 10^7$, for Raman scattering (see also Fig. 4), and as $G_{FWM} \sim |M_{2,2}|^2 \sim 10^{14}$, for degenerate four-wave mixing. According to Fig. 3, the local field intensity in the hot spots can approach the magnitude 10^5 so that the enhancement for nonlinear optical responses can be truly gigantic, up to 10^{10}, for Raman scattering, and up to 10^{20}, for four-wave mixing signals. With this level of enhancement, one can perform *nonlinear* spectroscopy of single molecules and nanocrystals. It is important that the enhancement can be obtained in the huge spectral range, from the near-UV to the far-infrared, which is a big virtue for spectroscopic studies of different molecules and nanocrystals. We also note that the field-enhancement provided by semicontinuous metal films can be used for various photo-biological and photo-chemical processes.

---

[1] D. J. Bergman and D. Stroud. In: *Solid State Physics* **46**, 147, Academic Press, Inc., New York (1992).

[2] V. M. Shalaev, *Nonlinear Optics Of Random Media: Fractal Composites and Metal-Dielectric Films* (Springer, Berlin Heidelberg, 2000).

[3] A. K. Sarychev and V. M.Shalaev, *Physics Reports* **335**, 275 (2000).

[4] D. Stauffer and A. Aharony, *Introduction to Percolation Theory*, 2 ed., Taylor and Francis, Philadelphia (1991).

[5] S. Grésillon, L. Aigouy, A.C. Boccara, J.C. Rivoal, X. Quelin, C. Desmarest, P. Gadenne, V. A. Shubin, A. K. Sarychev, and V. M. Shalaev, *Phys. Rev. Lett.* **82**, 4520 (1999).

[6] A. K. Sarychev, V. A. Shubin and V. M. Shalaev, *Phys. Rev. B* **60**, 16389 (1999); A. K. Sarychev and V. M. Shalaev, *Physica A* **266**, 115 (1999); V. M. Shalaev and A. K. Sarychev, *Phys. Rev. B* **57**, 13265 (1998); A. K. Sarychev, V. A. Shubin, and V. M. Shalaev, *Phys. Rev. E* **59**, 7239 (1999).

[7] R. W. Boyd, *Nonlinear Optics*, Academic Press Inc., New York (1992).